

10-2006

Experimentally Derived Resistivity for Dielectric Samples from the CRRES Internal Discharge Monitor

Nelson W. Green

A. Robb Frederickson

JR Dennison

Utah State University

Follow this and additional works at: http://digitalcommons.usu.edu/physics_facpub

 Part of the [Physics Commons](#)

Recommended Citation

Nelson W. Green, A. Robb Frederickson and JR Dennison, "Charge Storage Measurements of Resistivity for Dielectric Samples from the CRRES Internal Discharge Monitor," *IEEE Transaction on Plasma Science*, 34(5) October 2006, 1973-1978

This Article is brought to you for free and open access by the Physics at DigitalCommons@USU. It has been accepted for inclusion in All Physics Faculty Publications by an authorized administrator of DigitalCommons@USU. For more information, please contact dylan.burns@usu.edu.



EXPERIMENTALLY DERIVED RESISTIVITY FOR DIELECTRIC SAMPLES FROM THE CRRES INTERNAL DISCHARGE MONITOR

Nelson W. Green, A. Robb Frederickson, and J. R. Dennison

Abstract— Resistivity values were experimentally determined using charge storage methods for six samples remaining from the construction of the Internal Discharge Monitor (IDM) flown on the Combined Release and Radiation Effects Satellite (CRRES). Three tests were performed over a period of three to five weeks each in a vacuum of $\sim 5 \times 10^{-6}$ torr with an average temperature of ~ 25 °C to simulate a space environment. Samples tested included FR4, PTFE, and alumina with copper electrodes attached to one or more of the sample surfaces. FR4 circuit board material was found to have a dark current resistivity of $\sim 1 \times 10^{18}$ Ω -cm and a moderately high polarization current. Fiber filled PTFE exhibited little polarization current and a dark current resistivity of $\sim 3 \times 10^{20}$ Ω -cm. Alumina had a measured dark current resistivity of $\sim 3 \cdot 10^{17}$ Ω -cm, with a very large and more rapid polarization. Experimentally determined resistivity values were two to three orders of magnitude more than found using standard ASTM test methods. The one minute wait time suggested for the standard ASTM tests is much shorter than the measured polarization current decay times for each sample indicating that the primary currents used to determine ASTM resistivity are caused by the polarization of molecules in the applied electric field rather than charge transport through the bulk of the dielectric. Testing over much longer periods of time in vacuum is required to allow this polarization current to decay away and to allow the observation of charged particles transport through a dielectric material. Application of a simple physics-based model allows separation of the polarization current and dark current components from long duration measurements of resistivity over day- to month-long time scales. Model parameters are directly related to the magnitude of charge transfer and storage and the rate of charge transport.

Index Terms— Materials Testing, Resistivity, Conductivity, Dielectric, Spacecraft Charging, Space Environment Effects.

Manuscript received December 1, 2005. Support for the research was provided primarily from the NASA Space and Environments Effects Program.

N. W. Green is an Associate Engineer with the Reliability Engineering Office of the Jet Propulsion Laboratory, California Institute of Technology, Pasadena CA 91109-8099, (phone: 818-393-6323, fax: 818-393-0351, e-mail: Nelson.W.Green@jpl.nasa.gov).

A. R. Frederickson was a Principle Research Scientist with the Reliability Engineering Office of the Jet Propulsion Laboratory, California Institute of Technology, Pasadena CA 91109-8099. Dr. Frederickson passed away in April 2004.

J. R. Dennison is with the Physics Department, Utah State University, Logan, UT 84322-4415 USA, (phone: 435-797-2936; fax: 435-797-2492; e-mail: JR.Dennison@usu.edu).

I. INTRODUCTION

Standard constant-voltage ASTM test methods for measuring very high dielectric bulk resistivity [1], [2] do not provide accurate values for dielectrics appropriate for use in spacecraft deep dielectric charging applications [3]-[5]. These standard methods rely on electrometer measurements of current, voltage or resistance and are typically instrumentation resolution limited to accurate measurements of resistivities of less than 10^{12} to 10^{17} Ω -cm [1], [4], [5]. Inconsistencies in sample humidity, sample temperature, initial voltages and other factors from such tests cause significant variability in results [1]. Further, the duration of standard tests are short enough that the primary currents used to determine resistivity are often caused by the polarization of molecules by the applied electric field rather than by charge transport through the bulk of the dielectric [4]-[7]. Testing over much longer periods of time in a well-controlled vacuum environment is required to allow this polarization current to become small so that accurate observation of the more relevant charged particle transport through a dielectric material is possible. For space applications this is particularly important since dielectrics on the spacecraft will be exposed to space plasmas and radiation for months or years. Unless dissipated by leakage through the dielectric, charge will build up within the dielectric inducing large electric fields that can lead to dielectric breakdown and potentially harmful ESD pulses.

Selected samples remaining from the Internal Discharge Monitor (IDM) experiment on the CRRES satellite [8], [9] were tested for charge storage for NASA at the Jet Propulsion Laboratory. The sample set on CRRES was chosen to cover a range of dark current resistivity values and polarization magnitudes and rates. Hence, the set provides an excellent test bed for both the charge storage method of resistivity measurements and behavior of dielectrics in the space environment. By measuring the decay of stored charge in these dielectric samples, more accurate and appropriate resistivity values for the sample materials have been determined. Preliminary measurements of resistivities measured with the charge storage method for similar samples were shown to be critical in accurate modeling of the discharge pulsing of samples during the CRRES mission [10], [11]. The new resistivity values reported here are expected to further enhance the usefulness of the knowledge gained from

TABLE 1. LIST OF SAMPLES WITH CRRES IDM CHANNEL REFERENCE

Material	Thickness (cm)	Electrode	IDM Channel	Material Properties (ASTM Standard) [1]				
				(D150) ϵ_r	(D 257) ρ_{ASTM} ($\Omega \cdot \text{cm}$)	(D 150) $\delta_{1\text{MHz}}$	(D 149) E_S (MV/m)	
PTFE	0.229	Dual	11	2.1	1×10^{18}	0.0003	20	
PTFE*	0.229	Back	16	@ 1 MHz				
FR4*	0.119	Back	15	5.4	$>10^9$	0.035	27	
FR4	0.119	Back	15					@ 1 kHz
FR4	0.317	Dual	8					@ 1 kHz
FR4	0.317	Back	4,12					@ 1 kHz
Alumina*	0.102	Back	7	9.6	1×10^{14}	0.001	9.8	
				@ 1 MHz	@ 1 MHz	@ 1 MHz		

* Full analysis presented in this paper.

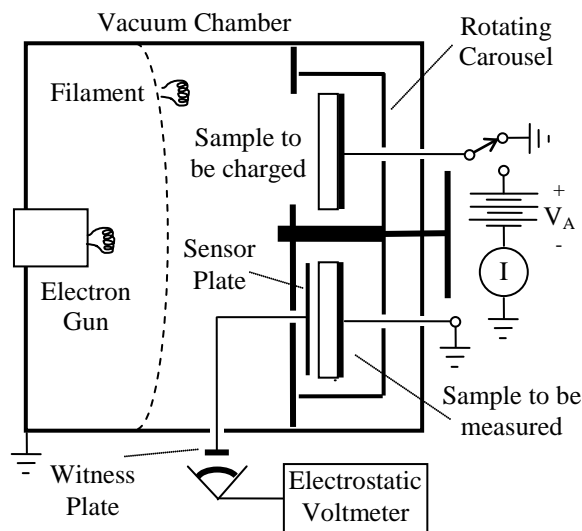


Fig. 1. Diagram of vacuum chamber arrangement as used while testing the CRRES IDM samples.

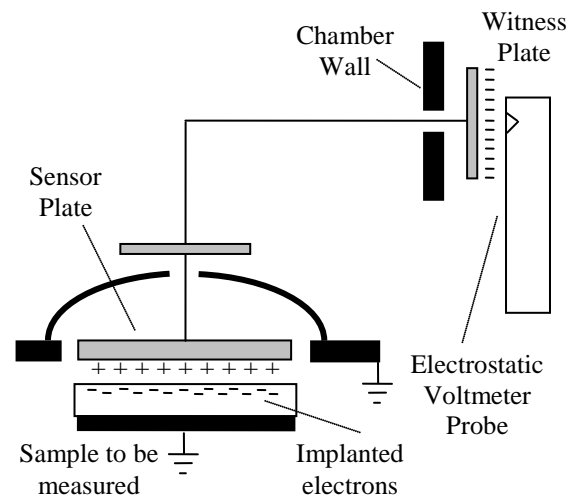


Fig. 2. Detail of the capacitive measurement system used to measure sample surface potential

the IDM experiment by producing experimental resistivity values for several of the samples.

Samples tested were 5x5 cm squares with copper electrodes on one or both surfaces. Materials included fiber-filled PTFE, Micaply FR4, and alumina (Al_2O_3) [8]. Three sets of tests were performed over a period of three to five weeks each in a vacuum of $\sim 5 \times 10^{-6}$ torr to simulate a space environment. **Sample temperature was not closely monitored, but an average temperature of 25 °C (laboratory room temperature) is assumed. Though the influence of temperature on dielectric resistivity is not fully understood and should be addressed in future work, the variance in laboratory temperature over the duration of the test was small enough to be ignored.**

Details for each sample, including standard ASTM material properties of dielectric constant, ϵ_r , resistivity, ρ , loss tangent at 1 MHz, δ , and the breakdown electric field strength, E_S are given in Table 1. Also provided is the CRRES IDM channel used to document the in flight pulse history for each sample as given in the references [10], [12], [13].

II. TEST PROCEDURE

Samples were mounted on a circular carousel (Fig. 1) inserted into a vacuum chamber behind a metallic plate with a single opening into the interior. This metal plate, referred to as the shutter, allowed each sample to be charged individually while all others were shielded from electron exposure. An electrically isolated sensor plate was mounted through a second opening in the shutter and connected via an electrical feedthrough to a smaller witness plate mounted outside of the vacuum chamber. This system of plates was used as a capacitive divider to measure sample surface potential (Fig. 2). To make each measurement, the isolated plate was allowed to float from ground while facing a grounded reference plate mounted on the circular carousel within the vacuum chamber. The floating system was then briefly grounded and the electrostatic voltmeter (Trek model 341) used to measure induced voltages on the floating sensor system was zeroed. To measure surface potential, each sample was then rotated

beneath the sensor plate and the induced change in potential on the witness plate was recorded. To relate these induced potentials to sample surface potentials, a coefficient was experimentally determined prior to the beginning of the experiment by applying a known potential of a few hundred volts to each sample while it was placed beneath the shutter mounted sensor plate. The coefficient obtained was the known applied voltage divided by the measured change in the potential on the witness plate. Typical coefficient values were between four and ten depending mainly on sample mounting geometry.

The isolated sensor plate, and the dielectric used to hold it in place on the shutter, was shielded from electron exposure by a grounded metallic cap and a series of baffles. To protect the electrostatic voltmeter, the floating sensor system was externally hard grounded when the electron gun was operated. Measurements represented an average surface potential over an area approximately equal to the 19 cm² surface area of the sensor plate. Connections to the electrodes on the back of each sample were brought through the chamber door for individual control or monitoring of each sample when charging.

Samples were charged with electrons by one of two methods: placing a positive potential of approximately 700 volts on each sample and attracting thermionically generated electrons from an energized filament near ground potential, or by floating the energized filament in an electron gun head at negative 15 to 35 kV compared to the grounded samples. In either case, the energy of incident electrons was roughly equal to the difference between the filament and the sample potentials. For the three samples analyzed fully in this paper, the former method was utilized with the filament adjusted to produce a current density of approximately 1 nA/cm² during the 90 second exposure given to each sample.

Three charging runs lasting for 20, 25, and 35 days respectively were performed with the CRRES IDM samples. Two charging runs were conducted successively after allowing the samples to outgas and dry out in vacuum for four days. The third run was performed on the same samples after approximately two months at atmosphere, after sitting at vacuum for two days. Measurements of the surface potentials were taken initially every few minutes, but as the changes between successive measurements became smaller, the interval between measurements increased first to hours then to days.

Further details of the instrumentation and test methods are found in references [4], [6]-[8], [11], [14], [15]].

III. RESISTIVITY MODEL

Since the actual amount of charged particles implanted near the surface of the materials could not be measured directly, each sample's surface potential was monitored to observe the changes in the electric field due to polarization of the material and, ultimately, dark current conduction of charge through the dielectric. A relatively rapid initial drop in the surface potential was expected for each sample due to dielectric polarization in the sample material. This initial decrease in potential was found to vary widely due to material properties. As any polar molecules in the material rotated to

align with the electric field created by the charges near the surface of the sample, or migrate within the dielectric to interfaces, they created a polarization electric field in opposition to that formed by the incident electrons. Since the measured surface potential was dependent on electric field strength from the sample, the opposing field reduced the measured voltage without necessarily indicating a reduction in the number of charged particles embedded in the sample. Simultaneously, charged particles may have been conducted through the material, but the majority of the short-term change in surface potential for high resistivity materials was thought to be through polarization of the sample material. As polarization reached saturation, further change in surface potential due to this effect became negligible and any further change was due to a reduction in the number of charged particles remaining near the surface of the charged sample. The charged particles that left the surface moved into the dielectric material filling electron traps or conducting through the material to ground. The dark current resistivity of the material was determined by the rate of charged particle transport, in the long-term asymptotic limit of charge storage measurements.

A simple model of the measured surface voltage as a function of elapsed time for the charge storage method $V_{CS}(t)$ in terms of the initial and final surface voltages (V_o and V_∞) and initial and final relative permittivities (ϵ_r^o and ϵ_r^∞ , where $\epsilon_o=8.854 \cdot 10^{-12}$ F/m is the permittivity of free space, ϵ is the permittivity in a dielectric medium, and $\epsilon_r \equiv \epsilon/\epsilon_o$ is the relative permittivity) predicts [4], [5]

$$V_{CS}(t; V_o, V_\infty, \epsilon_r^o, \epsilon_r^\infty, \rho_{DC}, \tau_p) = \frac{(\epsilon_r^o \cdot V_o - \epsilon_r^\infty \cdot V_\infty) e^{-t/\rho_{DC} \epsilon_o \epsilon_r(t)} + \epsilon_r^\infty \cdot V_\infty}{\epsilon_r(t)} \quad (1)$$

with $\epsilon_r(t) = (\epsilon_r^o - \epsilon_r^\infty) e^{-t/\tau_p} + \epsilon_r^\infty$

The polarization decay time, τ_p , measures the rate of the response of the medium to an applied electric field, and can be thought of as the rate at which the dipoles align within the material to the electric field E . It is the time it takes for the bound surface charge to increase to $(1-1/e)$ (or 63%) of its final value [5]. The charge storage decay time, τ_{DC} , is the time it takes for the free surface charge to drop to $1/e$ (or 37%) of its initial value and is directly proportional to the dark current resistivity $\tau_{DC}(t) = \rho_{DC} \epsilon_o \epsilon_r(t)$. Note that in this simple model the polarization decay time, dark current decay time, and resistivity are all intrinsic material properties independent of surface area or thickness. If there is no initial polarization, $\epsilon_r^o=1$. If there are no free charges trapped within the dielectric as it is transported through the material and $t \rightarrow \infty$, then this results in a residual potential, $V_\infty=0$. In the limit of short time, with $\tau_{DC} \gg \tau_p$,

$$V_{CS}(t; V_o, \epsilon_r^o, \epsilon_r^\infty, \tau_p) \rightarrow V_o \cdot \epsilon_r^o \left[\epsilon_r^\infty + (\epsilon_r^o - \epsilon_r^\infty) e^{-t/\tau_p} \right]^{-1} \quad (2)$$

In the limit of long time, with $\tau_{DC} \gg \tau_p$,

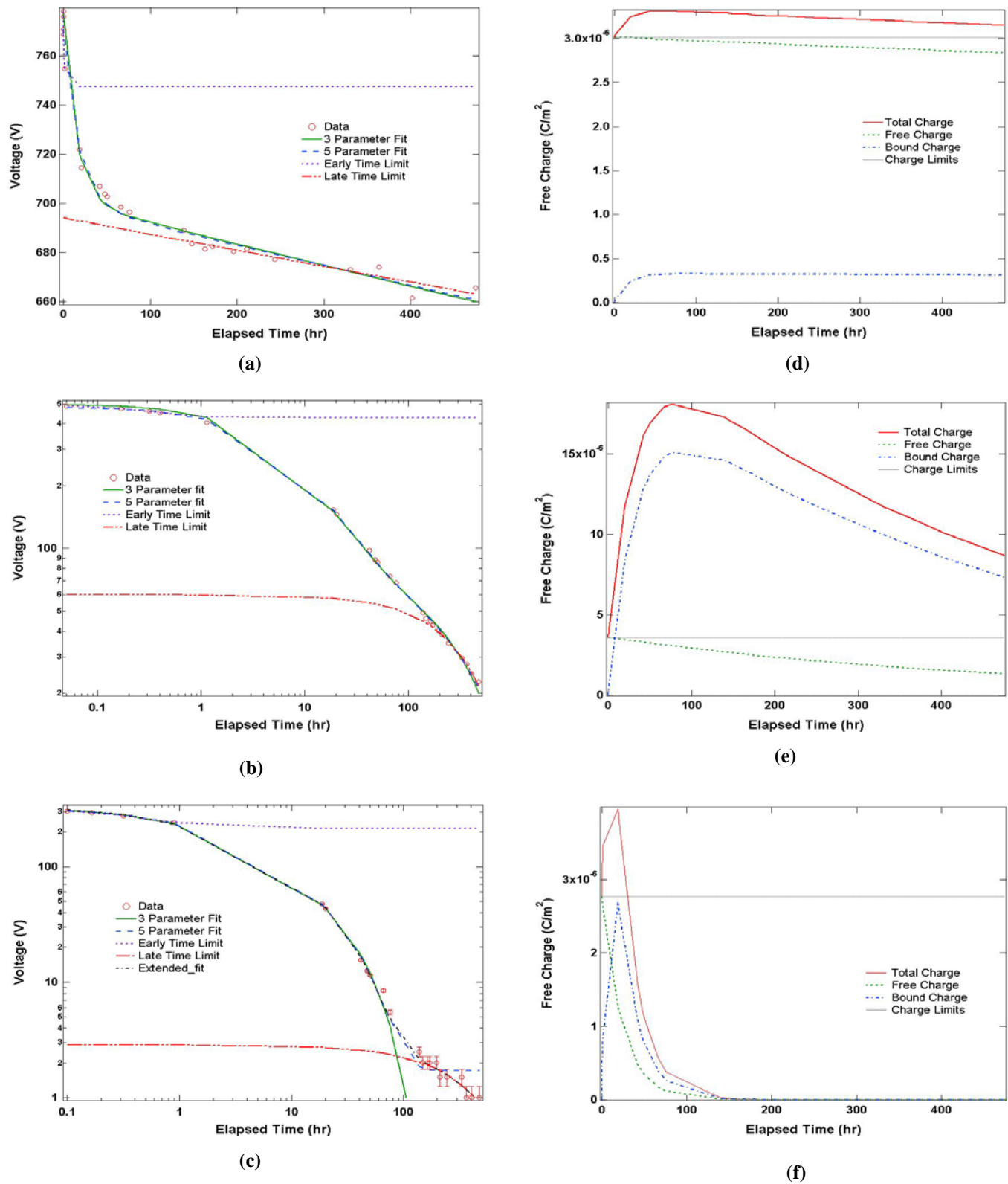


Fig. 3. Surface potentials functions of time for (a) PTFE, (b) FR4 and (c) alumina. Curves shows fits with three parameter fit using Equation (1) (dashdot), five parameter fit using Equation (1) (solid), early time limit model using Equation (2) (dashed) and the late time limit model with Equation (3) (dotted). Note the log-log plots of (b) and (c). For (c), there is also a modified 3-parameter fit with an additional decay mechanism. Charge as a function of elapsed time for (d) PTFE, (e) FR4 and (f) alumina. Plots are based on a three parameter fit using Equation (1). The initial and final values of the free charge from the fit are also shown.

TABLE 2. EXPERIMENTALLY DETERMINED RESISTIVITY VALUES FOR CRRES IDM SAMPLES*

Fit	Material	Thickness (cm)	ϵ_r^o	ϵ_r^∞	V_o (volt)	V_∞ (volt)	τ_p (hr)	τ_{DC} (day)	ρ_{DC} (Ω -cm)	ρ_{DC} / ρ_{ASTM}
3 parameter	PTFE	0.229	1.00	1.11	778	0	15.1	327	2.9×10^{20}	3×10^2
	FR4	0.317	1.00	6.54	484	0	34.7	19.9	3.0×10^{18}	$< 1 \times 10^9$
	Alumina	0.102	1.00	3.25	318	0	6.35	0.997	3.0×10^{17}	3×10^3
5 parameter	PTFE	0.229	1.01	1.12	778	28.8	15.1	313	2.7×10^{20}	3×10^2
	FR4	0.317	1.03	4.15	484	33.0	17.6	4.17	9.8×10^{17}	$< 1 \times 10^9$
	Alumina	0.102	1.02	2.88	318	1.74	7.03	0.864	2.9×10^{17}	3×10^3

$$V_{CS}^\infty(t; V_o, V_\infty, \epsilon_r^o, \epsilon_r^\infty, \rho_{DC}) = \frac{(\epsilon_r^o \cdot V_o - \epsilon_r^\infty \cdot V_\infty) e^{-t/\rho_{DC} \cdot \epsilon_r^o} + \epsilon_r^\infty \cdot V_\infty}{\epsilon_r^\infty} \quad (3)$$

IV. TEST RESULTS

A total of seven samples were charged and monitored for each of the three runs. Analyses of the data for three of the samples are presented below representing the general results for each sample material. For each analysis presented, the surface voltage measurements were fit using a least-squares fit method for:

- (i) the full data set using Eq. (1) with five fitting parameters, V_o , ϵ_r^o , ϵ_r^∞ , ρ_{DC} , and τ_p ,
- (ii) the full data set using Eq. (1) with three fitting parameters ϵ_r^∞ , ρ_{DC} , and τ_p , plus $\epsilon_r^o=1$ and $V_\infty=0$,
- (iii) the initial six data points using Eq. (2) with ϵ_r^∞ and τ_p as fitting parameters, and
- (iv) the last six data points using Eq. (3) with τ_{DC} as a fitting parameter.

In each case, V_o was set to the measured initial voltage. Results for the fits are listed in Table 2.

A. PTFE Charge Decay

The PTFE samples tested were a ‘‘Type 250’’ fiber-filled composite with a polytetrafluoroethylene matrix from the 3M Co. [8]. The decay pattern of the PTFE samples is significantly different from that of the other samples tested, and reflects the physical properties of the material. PTFE is known as a non-polar polymer, with a very low polarizability evidenced by its low dielectric constant of 2.1 [16]. The ratio of total charge to free charge in Figure 3b is indicative of this relatively small amount of polarization in PTFE. Because of the symmetry of the $(C_2F_4)_n$ PTFE monomer and the high affinity of fluorine for its electrons, the polymer has no permanent dipole moment and orientational polarization is not a major contributor [16]. Thus, polarization in PTFE results rapidly from induced dipoles through electronic and atomic polarization or more slowly due to defects through interfacial polarizability. Response of the long chain polymers and modifications of defects occurs slowly for PTFE, as evidenced by the relatively long polarization decay time $\tau_p \sim 15$ hr and the slow rise of the bound charge predicted in Figure 3b. PTFE has a very high dark current resistivity; this is evident in the very large value of the dark current decay constant $\tau_{DC} \sim 1$ yr

and in the slow decay of free charge predicted in Figure 3b. The measured ρ_{DC} is ~ 300 times larger than the ρ_{ASTM} value from standard handbooks [16]. The polarization decay constant corresponds to a resistivity of $\sim 6 \times 10^{17}$ Ω -cm, which is only slightly less than the ASTM value of $> 1 \times 10^{18}$ Ω -cm; this is consistent with the ASTM results when making measurements after only 1 min of voltage application, when the polarization current still dominates.

B. FR4 Charge Decay

The FR4 samples tested were a thermoset epoxy resin, fiberglass reinforced, Cu-clad laminate made by Micaply Co. [8]. FR4 is a standard designation for a broad class of composite materials typically used for printed circuit boards [17], [18]. The FR4 samples displayed intermediate charge storage characteristics. FR4 showed a fairly rapid initial drop in potential immediately after charging due to polarization. Response of the long chain polymers and modifications of defects of the FR4 composite were similar to those for PTFE, as evidenced by a similar long polarization decay time $\tau_p \sim 18$ hr and the slow rise of the bound charge predicted in Figure 4b. The higher ratio of total charge to free charge in Figure 4b is indicative of higher polarization than in PTFE and a relative dielectric constant of > 5 . The polymer and glass in FR4 have permanent dipoles—unlike PTFE—and the defect density is high due to the composite nature of the material. The unusually large ($\sim 8\%$) residual voltage, V_∞ , suggests that there is substantial residual charge in the FR4 sample. The FR4 has a dark current resistivity between the other two samples; this is evident in the intermediate dark current decay constant $\tau_{DC} \sim 4$ days and in the modest decay of free charge predicted in Figure 4b. Comparison of the measured ρ_{DC} to an ASTM standard value is not meaningful; the ASTM value listed [16] was not for the specific material tested but was rather from the FR4 standards [17], [18] that only specifies that ρ_{ASTM} not be less than 10^9 Ω -cm. Measurements with a different technique on a similar FR4 spacecraft material found a dark current resistivity of $\sim 2.12 \times 10^{17}$ Ω -cm [19], a factor of ~ 5 less than our measured ρ_{DC} .

C. Alumina Charge Decay

The alumina sample tested was a ~ 1 mm thick bulk alumina material, attached to a Cu substrate with silver-filled epoxy [8]. The alumina is believed to be Type II material with a Al_2O_3 content of $> 93\%$ [16]; this is reflected in the values listed in Table 1. The behavior of the alumina sample is

significantly different than the PTFE and FR4 polymer samples, due to its nature as a ceramic. Alumina has one of the highest dielectric constants of common ceramics, with a value of about 10. This follows mostly from the large permanent dipole moment of the Al_2O_3 unit cell that results from appreciable charge redistribution in the ionic/covalent bonds. The observation that the polarization decay constant of alumina is shorter than the polymers is to be expected as much of the polarization of alumina results from atomic polarizability due to distortion of the atoms within the unit cell. This leads to a large initial rise in the bound charge (see Figure 5b). However, the bound charge never exceeds the initial free charge because the polarization decay constant $\tau_p \sim 6$ hr is not too much shorter than τ_{DC} . This behavior is evident in the decay of the bound charge in Figure 5b. The alumina has a much lower dark current resistivity than either polymer; this is evident in the relatively small dark current decay constant $\tau_{DC} \sim 21$ hr and in the more rapid decay of free charge predicted in Figure 4b. The measured polarization and dark current resistivities are both approximately 3 orders of magnitude larger than the ASTM handbook value of $\sim 1 \times 10^{14} \Omega\text{-cm}$ [16]. The fact that $\rho_{ASTM} \ll \rho_p$ may reflect the sensitivity of alumina to the nature of defects of specific samples or to the humidity.

It is interesting to note that there is evidence of a small charge ($\sim 1\%$ of the initial free charge) that decays with a very long decay constant of >1 yr. This is apparent in the long time charge decay in Figure 5a. This term was modeled by modification of the exponential term of the numerator of Eq. (1) to include a second decay mechanism, $e^{-t/\tau_{DC}} \rightarrow [e^{-t/\tau_{DC}} + \alpha_H e^{-t/\tau_H}]$. A modified 3-parameter fit found $\epsilon_r^\infty = 2.84$, $\tau_p = 4.85$ hr, $\tau_{DC} = 19.8$ hr $\rightarrow \rho_{DC} = 2.6 \times 10^{17} \Omega\text{-cm}$ with $\alpha_H = 0.9\%$ and $\tau_H = 17.1$ days. We speculate that this may be related to the slow dissipation of charge trapped in deep level defect states of the alumina.

V. CONCLUSION

Laboratory testing has found that resistivity values for samples tested with the charge storage method were two to three orders of magnitude more than those given by standard ASTM test methods. The difference in measured resistivity is largely attributed to the dominance of polarization currents in the first hours after the application of an external electric field. When charge is deposited on the surface of dielectric samples held in a vacuum, the polarization current decays to an insignificant value, typically this effect is much faster than the dissipation of charge through the material. After the polarization current has been minimized, charge transport can more easily be observed and the resistivity calculated. The semi-empirical model applied in this paper has been found to accurately fit the data and to produce physically reasonable results based on the fitting parameters.

Three dielectric materials were tested and general results are listed in the analysis above. Fiber filled PTFE exhibited little polarization current and a dark current resistivity of $\sim 3 \times 10^{20} \Omega\text{-cm}$. FR4 circuit board material was found to have a dark current resistivity of $\sim 1 \times 10^{19} \Omega\text{-cm}$. Alumina had a measured dark current resistivity of $\sim 3 \cdot 10^{17} \Omega\text{-cm}$, with very large and more rapid polarization.

With these measured values, and others to come, the detailed analysis of the charging history of the CRRES IDM mission begun with great success by Frederickson and Brautigam [10] can be continued for more CRRES samples. It should be noted that the values calculated here are for samples that have not been exposed to radiation and have only been exposed to small amounts of low energy electrons. The resistivity of these materials may change, and change significantly, with exposure to space radiation. These results need to be verified through further analysis of the gathered data including that for other thicknesses and additional electrode configurations.

ACKNOWLEDGMENT

The authors would like to give thanks and acknowledgement to Jerilyn Brunson of Utah State University and Charles Benson of the Jet Propulsion Laboratory for their help and assistance in this effort. The research described in this paper was carried out at the Jet Propulsion Laboratory, California Institute of Technology, under a contract with the National Aeronautics and Space Administration.

REFERENCES

- [1] ASTM D257-99, "Standard Test Methods for DC Resistance or Conductance of Insulating Materials," American Society for Testing and Materials, West Conshohocken, PA, 1999.
- [2] IEC 93, "Methods of Test for Volume Resistivity and Surface Resistivity of Solid Electrical Insulating Materials," International Electrotechnical Commission Publication 93, Second Edition, 1980.
- [3] P. Swaminathan, A.R. Frederickson, J.R. Dennison, A. Sim, J. Brunson, and E. Crapo, "Comparison of Classical and Charge Storage Methods for Determining Conductivity of Thin Film Insulators," *Proceedings of the 8th Spacecraft Charging Technology Conference*, NASA Marshall Space Flight Center, Huntsville, Alabama, October 2003.
- [4] J.R. Dennison and A. R. Frederickson, "Comments on Engineering Design Guidelines: Resistivity Measurements Related to Spacecraft Charging," NASA Space Environments and Effects Program, Contract No. NAS8-02031, "Measurement of Charge Storage Decay Time and Resistivity of Spacecraft Insulators," April, 2002 to January, 2005.
- [5] J.R. Dennison, P. Swaminathan, R. Jost, J. Brunson, N. W. Green and A. R. Frederickson, "Proposed Modifications to Engineering Design Guidelines Related to Resistivity Measurements and Spacecraft Charging," *IEEE Transactions on Plasma Science*, to be published.
- [6] A. R. Frederickson and J. R. Dennison, "Measurement of Conductivity and Charge Storage in Insulators Related to Spacecraft Charging," *IEEE Transactions on Nuclear Science*, vol. 50, no. 6, pp. 2284-2291, December 2003.
- [7] A. R. Frederickson, C. E. Benson, and J. F. Bockman, "Measurement of Charge Storage and Leakage in Polyimides," *Nuclear Instruments and Methods in Physics Research B*, 208, pp. 454-460, 2003.
- [8] A. R. Frederickson, E. G. Mullen, K. J. Kerns, P. A. Robinson, and E. G. Holeman, "The CRRES IDM Spacecraft Experiment For Insulator Discharge Pulses," *IEEE Transactions on Nuclear Science*, vol. 40, no. 2, pp. 233-241, April 1993.
- [9] A. R. Frederickson, "Radiation-Induced Insulator discharge Pulses in the CRRES Internal Discharge Monitor Satellite Experiment," *IEEE Transactions on Nuclear Science*, vol. 38, no. 6, pp 1614-1621, Dec. 1991.
- [10] A. R. Frederickson and D. H. Brautigam, "Mining CRRES IDM Pulse Data and CRRES Environmental Data to Improve Spacecraft Charging/Discharging Models and Guidelines," NASA/CR-2004-213228. NASA Space Environments and Effects Program, Marshall Space Flight Center, June 2004.
- [11] J.R. Dennison, A.R. Frederickson and P. Swaminathan, "Charge Storage, Conductivity and Charge Profiles of Insulators As Related to Spacecraft Charging," *Proceedings of the 8th Spacecraft Charging Technology Conference*, NASA Marshall Space Flight Center, Huntsville, AL, October 2003.

- [12] A. R. Frederickson, A. C. Whittlesey, H. B. Garrett, "Comparing CRRES Internal Discharge Monitor Results with Ground Tests and Published Guidelines." *Proceedings of the 7th Spacecraft Charging Technology Conference*, ESA SP-476, Noordwijk, The Netherlands, April 2001.
- [13] A. R. Frederickson, E. G. Mullen, K. J. Kerns, P. A. Robinson, and E. G. Holeman, "The CRRES IDM Spacecraft Experiment For Insulator Discharge Pulses." *IEEE Transactions on Nuclear Science*, vol. 40, no. 2, pp. 233-241, April 1993.
- [14] J.R. Dennison, A. R. Frederickson, N. W. Green, P. Swaminathan, and J. Brunson, "Test Protocol for Charge Storage Methods," NASA Space Environments and Effects Program, Contract No. NAS8-02031, April, 2002 to January, 2005.
- [15] J.R. Dennison, A. R. Frederickson, N. W. Green, P. Swaminathan, and J. Brunson, "Measurement of Charge Storage Decay Time and Resistivity of Spacecraft Insulators," NASA Space Environments and Effects Program, Contract No. NAS8-02031, April, 2002 to January, 2005.
- [16] W. Tillar Shugg, *Handbook of Electrical and Electronic Insulating Materials*, 2nd Ed; *The Guide to Plastics* by the Editors of *Modern Plastics Encyclopedia*, McGraw Hill, Inc., N.Y., 1970.
- [17] ASTM D1867, "ASTM Standard for Copper-clad Thermoset Laminates" American Society for Testing and Materials, West Conshohocken, PA, 1999.
- [18] IPC Standard 4101A, "Specification for Base Materials for Rigid and Multilayer Printed Boards including Amendment 1," The Institute for Interconnecting and Packaging Electronic Circuits, Northbrook, IL, 1999.
- [19] R. M. Beilby, P. A. Morris, K. A. Ryden, D. J. Rodgers and J. Sorensen, "Determination of Conductivity Parameters of Dielectrics Used in Space Applications" *Proceedings of 2004 IEEE International Conference on Solid Dielectrics*, p. 936, 2004.